Blind Medical Image Watermarking with LWT – SVD for Telemedicine Applications

N.Venkatram, L.S.S.Reddy, P.V.V.Kishore
Department of ECM, CSE and ECE
KL University
Green Fields, Vaddeswaram, Guntur DT, Andhra Pradesh
INDIA
nvenkatran@kluniversity.in, lssreddy@kluniversity.in, pvvkishore@kluniversity.in

Abstract: - This paper highlights the extension of dwt-svd based image watermarking to medical images. In recent times internet has become a primary source of communication between the diagnostics center and the remote doctor located at some hospital. With the use of internet come the problem of data authenticity and the responsibility of the medical practitioner to preserve sensitive information of patients contained in the medical images related to that particular patient. Hence we have made an attempt to solve this problem by using dwt-svd based watermarking technique used for normal images. For medical images quality preservation is obligatory we have used 2D lifting wavelet transform (LWT) instead of dyadic 2D discrete wavelet transform. To test our algorithm we used computer tomography (CT) images as the original images. The watermark is chosen as patient picture which is hidden in a CT medical image while transmitting through internet. The results show that after attacks lwt-svd method gives satisfactory quality both visually and mathematically.

Key-Words: - Medical Image watermarking, Lifting Wavelet Transform, Singular Value Decomposition, Computer Tomography, lwt-svd watermarking.

1 Introduction

Image watermarking primary aim is to prevent digital images form copyright theft when transmitted over unsecured wireless networks and databases. Authentication of digital images is guaranteed by hiding copyright information image in the original digital image. Image watermarking is regularly used by today's internet users while posting images on the internet [1]-[3]. A digitally watermarked image should be imperceptible to the human preceptor while maintaining the quality of the watermark after extraction form the watermarked image. The challenge faced by the image processing research community is to strike a balance between these two watermarking processes along the amount of watermark information to be embedded in the original image [4].

The trickiest part in digital image watermarking processes is to hold the equilibrium between watermark embedding, watermark extraction and the amount of hidden watermark payload [5]. Maity et.al. [6] has discussed a wide range of watermarking techniques ranging from mathematical models to low cost intelligent soft computing techniques. The most popular technique for image watermarking is Discrete Cosine Transform (DCT) [7]. Constraints DCT is a modified version of DCT where watermark embedding consists of liner constraints among selected DCT coefficients. Another DCT watermarking defines circular detection regions in DCT domain for embedding. Spread spectrum (SS) based image watermarking is another most popular format for watermarking. In SS based watermarking a watermark is constructed as an independent and identically distributed (i.i.d.) Gaussian random vector that is imperceptibly inserted in a spread-spectrum-like fashion into the perceptually most significant spectral components of the data [8]. This system makes the watermark vigorous to signal processing operations (such as lossy compression, filtering, digital-analog and analog-digital conversion, re quantization, etc.), and common geometric transformations (such as cropping, scaling, translation, and rotation) provided that the original image is available and that it can be successfully registered against the transformed watermarked image.

The subsequent widely used process for image watermarking is discrete wavelet transform (DWT). In DWT based watermarking, the watermark bits are embedded in the middle-frequency subimage in the wavelet domain [9]. They further selected the appropriate dilation factor and filters in the

multiband wavelet transform to achieve better performance in terms of watermark invisibility and the robustness. In a DWT-based scheme, the DWT coefficients are modified with the data that represents the watermark. Emir Ganic et.at. present a hybrid scheme based on DWT and Singular Value Decomposition (SVD). After decomposing the cover image into four bands, SVD is applied to each band, and embed the same watermark data by modifying the singular values. Modification in all frequencies allows the development of a watermarking scheme that is robust to a wide range of attacks [10]-[11].

In recent years it has become a regular practise to send medical images through internet from the diagnostics centre to doctor. The sensitive medical information related to a patient traverses through unsecured networks and databases. This makes the medical images vulnerable to attacks which include tampering of images compromising the patient's information. Fig.1 shows the two ultrasound images one original breast cancer image and another tampered ultrasound image of the same patient. Images are courtesy of [12].
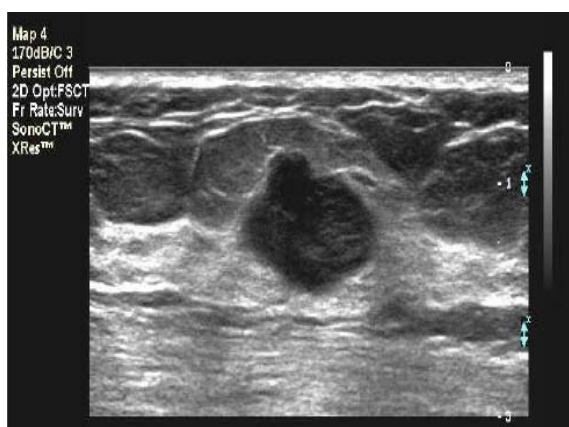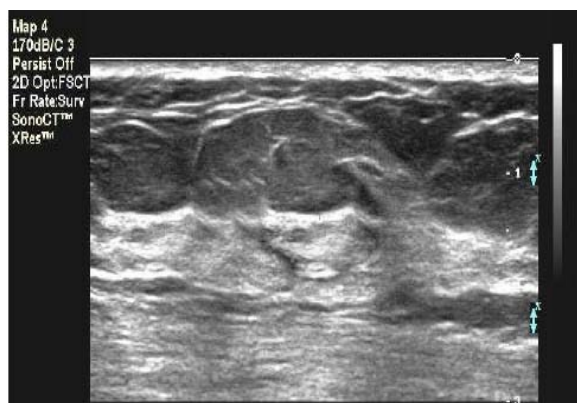

Fig.1 Breast Cancer of a patient

Fig.2 Tampered Image of the same patient as fig.1.

Lou et.al. [13] proposed a technique of pixel-value difference expansion. It proposes a multiple-layer data hiding technique in spatial domain. It utilizes a reduced difference expansion method to embed the bit stream in the least significant bits (LSBs) of the expanded differences. By using the reduced difference expansion method, we can embed a large amount of data in a medical image whose quality can also be maintained. Moreover, the original image can be restored after extracting the hidden data from the stegno image. Experimental results show that the proposed scheme provides higher embedding capacity at the same level image quality compared with Tai's [14] difference expansion method.

Lavanya et.al. proposed non region of interest (NROI) based medical image watermarking schemes [15] where the patient details are embedded in non-ROI region of an image. The encrypted image is divided into non overlapping tiles to identify region of interest and non-region of interest. In examination site examiner embeds patient details in non-ROI of encrypted image using a data-hiding key. With an encrypted image containing patient details, a receiver may first de tile and decrypt it using the encryption key, and the decrypted version is similar to the original image [16]-[17].

This research proposes to use an amalgam of wavelet transform [18]-[19] and Singular Value Decomposition for medical image watermarking. Recently watermarking techniques have gone hybrid. Hybrid watermarking schemes use mixture of two or three transformation in the watermarking process. SVD transform preserves minor transitions with largest changed singular values that occur during attacks. The basic process in DWT-SVD watermarking process lies in modifying the wavelet sub bands using singular values of binary watermark image[20]-[23].

A new improved watermarking scheme is proposed using lifting wavelet transform (LWT) [24] and SVD for medical images. The medical images of patients are watermarked with the image of that particular patient which is extracted at the doctor's end to identification. Lifting wavelets have distinctive advantage that is explored and is missed in traditional wavelet transform. With lifting wavelets the inverse transformation is undoing the operations of forward transform which reduce the artefacts during transformation. The rest of the paper is organized as follows. Section 2 and 3 gives

a brief introduction of lifting discrete wavelet transform and Singular Value Decomposition (SVD) techniques. Section 4 deals with the process of medical image watermarking using LWT-SVD and dewatermarking algorithm. Section 5 introduces measurable parameters that can judge the watermarking procedures. Results and discussion in section 6 provide insight into the use of hybrid multiresolution lifting wavelet transform and SVD for medical image watermarking. Finally conclusions are drawn on the medical image watermarking schemes using LWT-SVD technique in section 7.

2 Lifting Wavelet Transform (LWT)

Lifting wavelets come under the category of second generation wavelets that have distinctive advantages over traditional first generation wavelets. The lifting wavelets trim down the computing time and memory requirements as they adopt an in position realization of wavelet transform. Unlike traditional wavelets the computations for lifting wavelets are performed in integer domain rather than real domain. More over the inverse process in lifting wavelets is ruination of the processes performed during the forward transformation. This the main reason for choosing LWT [24] over traditional DWT [25]-[27] for medical image watermarking.

The Lifting Wavelet Transform (LWT) comprises of three basic steps which form the basis for integer transformations: split, predict and update as shown in figure 3.
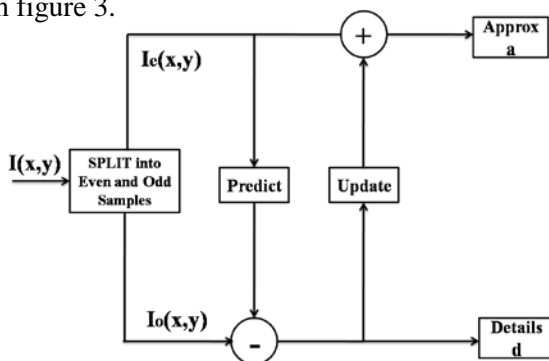

Fig. 3. Lifting Wavelet Forward Transform

Split – decompose the image $I(x, y)$ into even $I_e(x, y)$ and odd $I_o(x, y)$ polyphase components. The z-Transform of even polyphase component is expressed as

$$I_e(z_1, z_2) = \sum_{n=1}^{N} \sum_{m=1}^{M} I(2n_1, 2n_2) z_1^{-n_1} z_2^{-n_2} \quad (1)$$

and odd polyphase z-transform is expressed as

$$I_o(z_1, z_2) = \sum_{n=1}^{N} \sum_{m=1}^{M} I(2n_1 + 1, 2n_2 + 1) z_1^{-n_1} z_2^{-n_2} \quad (2)$$

The combination of predict operation and subtraction replaces the odd polyphase coefficient $I_o(z_1, z_2)$ with difference between the odd polyphase component $I_o(z_1, z_2)$ and predicted value $P[..]$. The prediction operation is applied on even polyphase components $I_e(z_1, z_2)$. In this case we simply consider the predictor as the average of two neighbouring even polyphase samples.

$$P[..] = \frac{1}{2}\left[I_e(z_1, z_2) + I_e(z_1 + 1, z_2 + 1)\right] \quad (3)$$

Where $I_e(z_1, z_2)$ and $I_e(z_1 + 1, z_2 + 1)$ are two successive samples in z domain and $I_e(n_1, n_2)$ and $I_e(n_1 + 1, n_2 + 1)$ are corresponding inverses in spatial domain. The detailed coefficients are computed using the expression

$$d(n_1, n_2) = I_o(n_1, n_2) - P[..] \quad (4)$$

The predication process produces details coefficients and the operation imply high pass filter. Update operator $U[..]$ updates the even polyphase samples $I_e(n_1, n_2)$ using the detailed coefficients computed $d(n_1, n_2)$ in the prediction stage. The update $U[..]$ is defined as a proportionality factor between the sum of approximate coefficients and mean of input matrix.

$$U[..] = \frac{\frac{1}{2}\left(\sum_{n_1, n_2} a(n_1, n_2)\right)}{\sum_{x, y} I(x, y)} \quad (5)$$

The update stage substitutes even samples $I_e(n_1, n_2)$ with

$$a(n_1, n_2) = I_e(n_1, n_2) + U[..] \quad (7)$$

$a(n_1, n_2)$ are approximate coefficients representing low frequency components of the original image $I(x, y)$. The inverse process is quite opposite to that of the forward transformation as shown in figure 4.
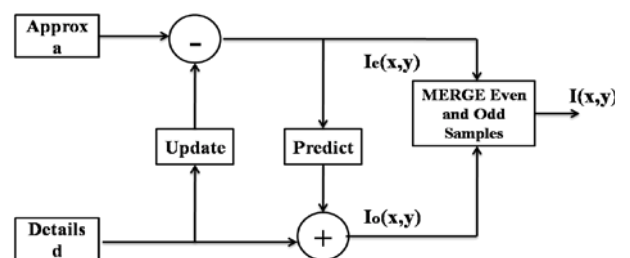

Fig.4. Reconstruction LWT

3 Singular Value Decomposition

Singular Value Decomposition (SVD) [20] is a mathematical tool used in matrix diagonalization to compute singular value matrices from a host matrix. SVD is widely used in watermarking because of the advantage it offers in hiding the watermark effectively when changes occur in large singular values. In watermarking SVD is used in combination with DWT [21]-[23] where watermark is embedded in the transform coefficients of the host image instead of pixels. A matrix in SVD is decomposed into three matrices. For an image matrix $I(x,y) \in \Re$ indicated as a real number $\Im$ of size $m \times n$ with $m \geq n$, the SVD is formulated as

$$\Im = U \Sigma V^T \tag{8}$$

Where U and V are orthogonal matrices of size $m \times r$ and $r \times n$ respectively. Σ is a diagonal matrix of size $r \times r$ containing singular values of $\Im$. Here r is the rank of input matrix $\Im$.

$$\Sigma = \begin{bmatrix} \sigma_{11} & 0 & & . & . & . & 0 & 0 \\ 0 & \sigma_{22} & & . & . & . & 0 & 0 \\ 0 & 0 & \sigma_{33} & . & . & & 0 & 0 \\ . & . & & . & . & & 0 & 0 \\ . & . & & . & . & & 0 & 0 \\ 0 & 0 & & . & . & . & \sigma_{r_1 r_2 -1} & 0 \\ 0 & 0 & & . & . & . & 0 & \sigma_{r_1 r_2} \end{bmatrix} \tag{9}$$

Where $\sigma_i 's$ singular values of $\Im$ and their number is equal to rank of $\Im$. SVD offer distinct advantages such as efficiently representing indispensable algebraic properties of the image, where singular values $\Sigma = \{\sigma_{11}, \sigma_{22}, \sigma_{33}, ...\sigma_{r_1 r_2 -1}, \sigma_{r_1 r_2}\}$ correspond to pixel brightness and image geometry features are modelled with singular vectors U and V. Moreover singular values are completely stable in the sense that a small commotion to the watermarked image will not appreciably modify the singular values, preserving the quality of the watermarked image and its contents for extraction.

4 Proposed LWT–SVD watermarking

In this work, Lifting Wavelet Transform (LWT) and singular value decomposition are used together to accomplish the task of watermarking medical images with patients image. The watermarking embedding and extraction procedures are illustrated in figure 5 and figure 6 respectively. This research is an attempt to insert patient's image of size 64×64 into their medical images of size 256×256 instead of binary data of the patient as done by most of the researchers. This presents quite a challenging task to retain the medical information after watermarking and extraction of patient's image at the doctor's end even after attacks.
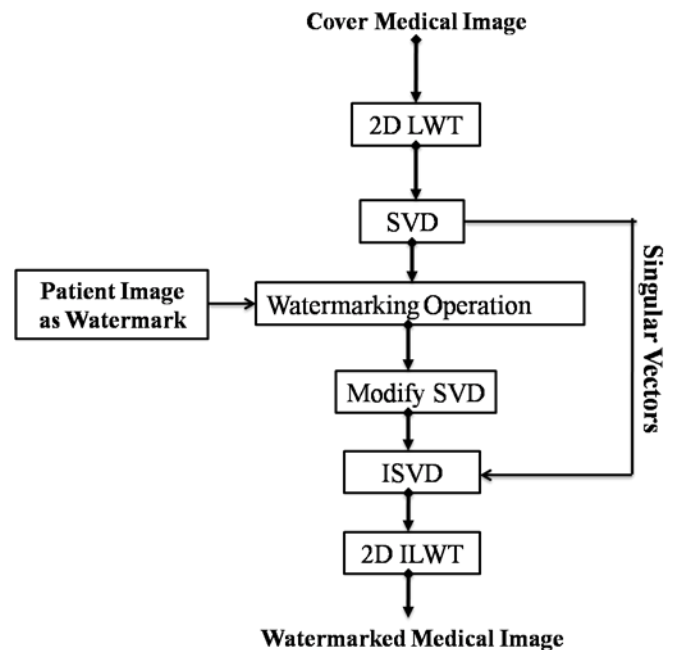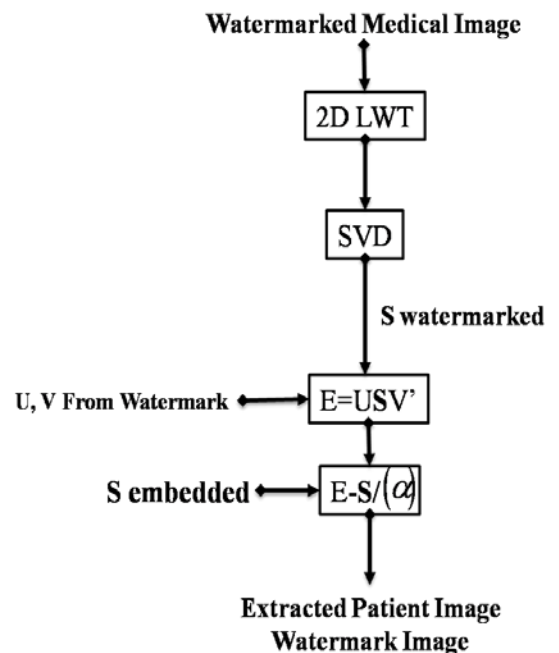
Fig.5.Watermak Embedding Algorithm

Fig.6.Watermak Extraction Algorithm

4.1 Medical Image Watermarking Process

Medical Images are watermarked with their corresponding patient image is accomplished using the following steps.

S1. Carry out 1st level 2D Lifting Wavelet Transform (LWT) on the Medical Image (Cover Image) and decompose in to following sub-bands (LL, LH, HL, HH).

S2. Apply SVD to all sub-bands

$$S^{(n)} = U^{(n)}\Sigma^{(n)}V^{(n)T} \qquad (10)$$

Where n is the sub-band pointer i.e. LL, LH, HL and HH.

S3. Modify the sub-bands singular values $\Sigma^{(n)}$ by inserting the watermark i.e. patient image pixels directly using the expression

$$WM^{(n)} = \Sigma^{(n)} + \alpha w^{(p)} \qquad (11)$$

$w^{(p)}$ Corresponds to pixels values in the watermark. Here α can take values in the range 0.007 to 0.07 determines the strength of the watermark.

S4. Apply inverse singular value decomposition using the singular vectors $U^{(n)} \& V^{(n)T}$ from step 2. The latest modified sub-bands are produced using the formulation

$$W^{(n)} = U^{(n)}WM^{(n)}V^{(n)T} \qquad (12)$$

Where $W^{(n)}$ modified sub-bands.

S5. Finally, assemble all the modifies sub-bands and apply inverse 2D Lifting Wavelet Transform (ILWT) and is formulated as

$$W^{MI} = \left(W^{(n)}\right)^{-1} \qquad (13)$$

$W^{(n)}$ represents 4 sub-bands for n=1, LL, LH, HL, HH. W^{MI} is the watermarked medical image.

4.2 Watermark Patient Image Extraction Process

The watermarked medical image W^{MI} is sent to remotely on the unsecured internet to a doctor. At the doctor's end the system decouples the attacked watermarked medical image form the watermark for authentication that these medical images belong to that particular patient. The following steps are followed at the doctor's side to extract the watermark patient image.

S1. The possibly attacked watermark medical image is treated with 2D Lifting wavelet transform (LWT) and decomposed to level 1 with 4 sub-bands LL, LH, HL and HH.

S2. Apply SVD to all sub-bands.

$$E_p^{(n)} = U_e^{(n)}\Sigma_e^{(n)}V_e^{(n)T} \qquad (14)$$

S3. Apply inverse SVD but with orthogonal vectors derived from watermarking process.

$$E^{(n)} = U^{(n)}\Sigma_e^{(n)}V^{(n)T} \qquad (15)$$

S4. Extract the watermark E^{PI} patient image from the watermarked medical image using the following formulation

$$E^{PI} = \frac{E^{(n)} - \Sigma_e^{(n)}}{\alpha} \qquad (16)$$

E^{PI} is the extracted patient image watermark in level n.

5 Results and Discussion

This method is implemented on MATLAB 13.0.1 software with three different types of medical images which are considered as cover images. MRI, CT and Ultrasound medical images are used as cover images of standard resolution 256×256. Watermark is a patient image of resolution 64×64. This method does not put a constraint on patient watermark image resolution which can be of the same size as the medical cover image. Since medical images are gray scale images, it is intended to consider grayscale patient image as watermark. The scaling factor α=0.07 is used for watermarking in our experiments. Other scaling factors that can be used 0.05, 0.02 or two different scaling factors for approximate coefficients and detail coefficients.

The performance of the proposed medical image watermarking is judged by computing peak signal to noise ratio (psnr) and normalized cross correlation coefficient (ncc). These parameters will decide the robustness of the watermarking method using 2D LWT-SVD method. Watermarking of medical images is quite sensitive process as the medical images contain information related to a disease of human subject. Corruption of the original medical image by watermarking process should be within the permissible limits of human perception. The visual sensitivity of the watermarked and extracted images is mathematically represented by calculating psnr and ncc.

5.1 Embedded Peak Signal to Noise Ratio (psnr)

Embedded psnr [28] is the measure of peak error between original image and watermarked image and is formulated as

$$psnr = 10\log_{10}\left(\frac{MN\left(\max(\max(I^M(x,y))^2\right)}{\sum_{x \in N}\sum_{y \in M}\left(I^M(x,y) - W^{MI}\right)^2}\right) \qquad (17)$$

Where N and M represent image resolution. $I^M(x,y)$ is the original medical image and W^{MI} is the watermarked medical image. psnr is the peak signal to noise ratio in db which range between 40db to 60 db generally for good watermarking.

5.2 Extracted Normalized Cross Correlation Coefficient (ncc)

Normalized cross correlation is mostly used by pattern recognition research for measuring similarity between a query image and the images from the database. The cross correlation is normalized by subtracting the mean and dividing by standard deviation. Embedded normalized cross correlation coefficient gives the measure of closeness between watermarked image and original medical image.

$$ncc = \frac{\sum_{x \in N} \sum_{y \in M} I^M(x,y) \times W^{MI}(x,y)}{\sqrt{\sum_{x \in N} \sum_{y \in M} \left[I^M(x,y) \right]^2} \sqrt{\sum_{x \in N} \sum_{y \in M} \left[W^{MI}(x,y) \right]^2}} \quad (18)$$

The values of normalized cross correlation coefficients (ncc) range from 0 to 1. Larger values of ncc are preferred for better watermarking.
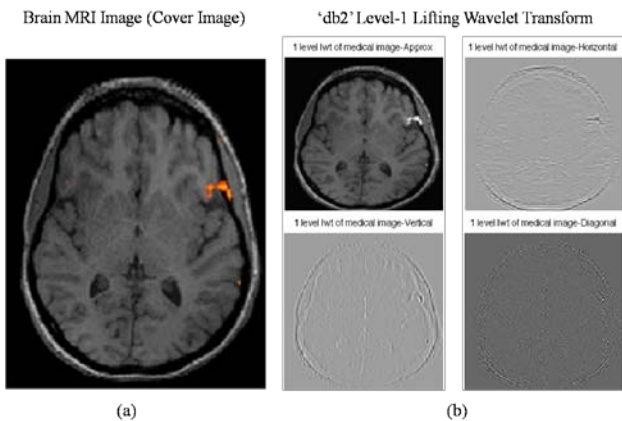

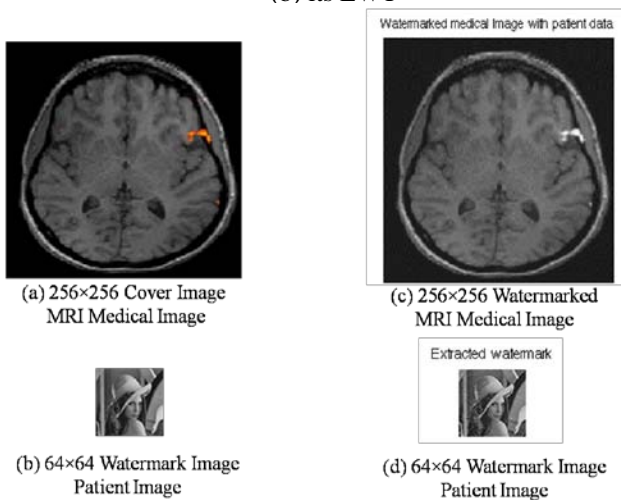Fig.7. Lifting Wavelet Using 'db2' (a) Brain MRI Image (b) its LWT

Fig.8. (a) MRI Cover Image (b) Patient Image Watermark (c) Watermarked MRI Image With Patient Image using LWT-SVD (d) Extracted Watermark

Figure 7 shows brain MRI of a patient along with its lifting wavelet transform. LWT decomposes using debauches2 (db2) mother wavelet to a level-1 decomposition. MRI brain medical image(256×256) is used as cover image for watermarking in figure 8(a) and lena image is used as patient image(64×64) in figure 8(b).

LWT-SVD watermarking procedure as proposed embeds patient image into the watermarked brain MRI image as shown in figure 8(c). Figure 8(d) shows the extracted watermark of patient image. From figure 8 it can be observed that the watermarked image and extracted image match strongly enough as per human visual system. This shows the robustness of LWT-SVD algorithm. Similar results can be obtained using Computer Tomography (CT) and Ultrasound (US) Medical images as cover images. The results for CT and US are shown in figures 9, 10, 11 and 12 respectively.
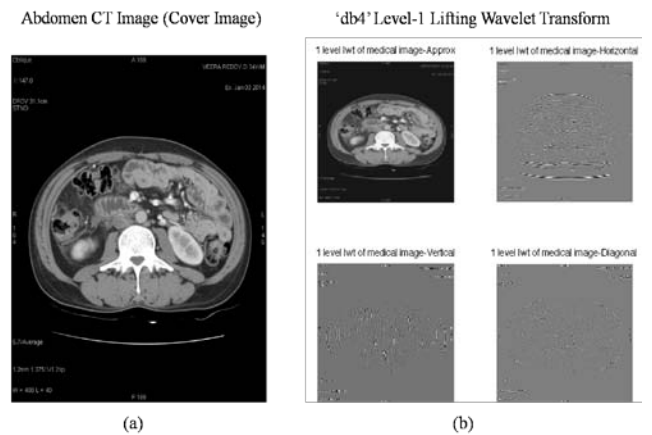

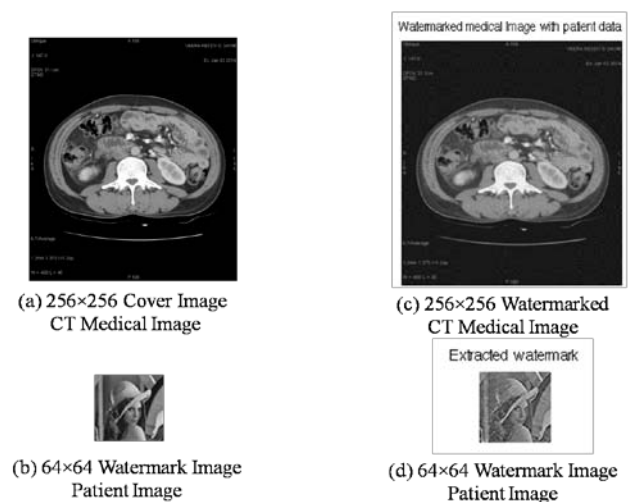Fig.9. Lifting Wavelet using 'db4' Mother wavelet (a) CT Medical Cover Image (b) its LWT

Fig10. (a) CT Cover Image (b) Patient Image Watermark (c) Watermarked CT Image With Patient Image using LWT-SVD (d) Extracted Watermark
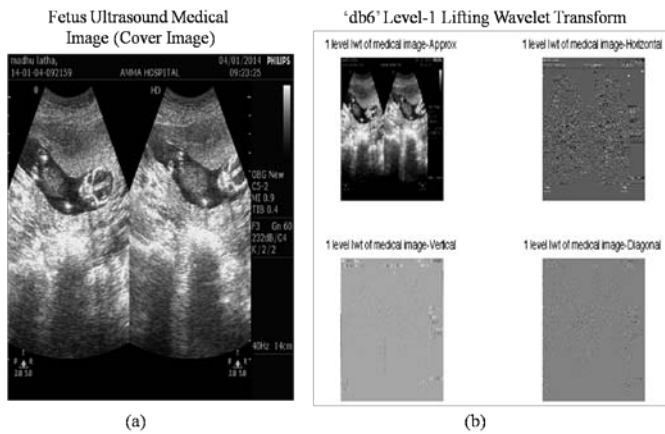
Fig.11. Lifting Wavelet using 'db6' Mother wavelet (a) US Medical Cover Image (b) its LWT
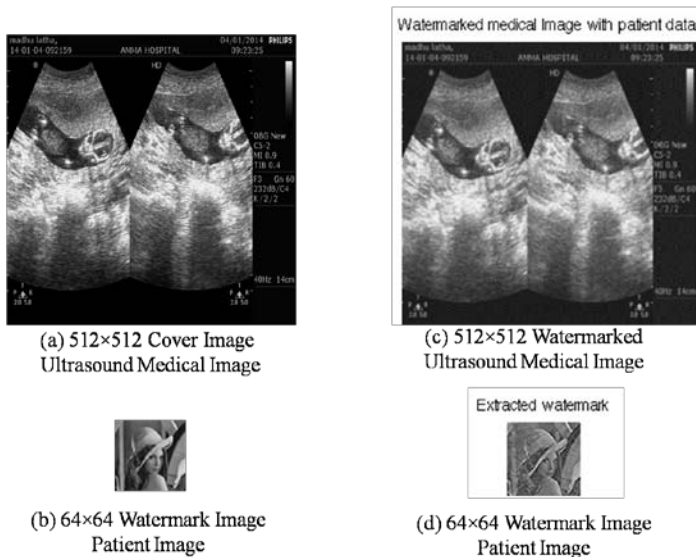

Fig12. (a) US Cover Image (b) Patient Image Watermark (c) Watermarked CT Image With Patient Image using LWT-SVD (d) Extracted Watermark

The CT and US medical cover images are watermarked using mother wavelets 'db4' and 'db6' lifting scheme. Visually comparing the watermarked medical images from figures 8, 10 and 12(c) with patient image reveal that there is remarkably no deviation in case of MRI and CT for 'db2' and 'db4' wavelets except for a small one in case of US medical image from its watermark US image for 'db6' mother wavelet. Results are also formulated using equations 17 and 18 in Table-I for the embedded watermark and original medical image for all three different medical images. The data interpretation highlights the effectiveness of the LWT-SVD watermarking procedure for medical image watermarking with patient image as payload.

Table-I

Cover Medical Image	PSNR(db)	NCC
MRI	46.8998	0.9869
CT	47.3565	0.9899
Ultrasound(US)	45.3454	0.9768

From Table-I psnr in db for MRI, CT and US watermarks are 46.8998db, 47.3565db and 45.3454db respectively. Comparing with psnr values of dwt-svd watermarking in [22] our proposed lwt-svd on medical images are almost within the prescribed values of watermarking [22]. Normalized Cross Correlation (ncc) coefficient is good for MRI and CT with 0.9869 and 0.9899 compared to US at 0.9768. Again the values are within the permissible range as proposed by lwt-svd watermarking and compared to results in [22]. From figures 8(c), 10(c) and 12(c) it can be visually confirmed that the lwt-svd produces high quality medical watermarked images which are loaded with medical information as that of original medical images. The extracted watermark images are shown in figures 8(d), 10(d) and 12(d) which are extracted from MRI,CT and US images using 'db2', 'bd4' and 'db6' mother wavelets. The extracted watermark from MRI watermarked image using 'db2' is of high quality compared to watermark extracts from CT and US using 'db4' and 'db6'.

The watermarked medical images are transmitted on unsecured networks making them prone to attacks from various unlawful elements present on the network. Hence to simulate attack environment on the internet for our research we modeled six types of commonly used attacks with different values making the total number of attacks to fifteen. We then compute normalized cross correlation coefficient form equation 18 for the extracted watermarked images. The values are put up in Table-II.

Generally the ncc coefficient for better watermark is something above 0.75[22]. For remarkably excellent correlation the value of ncc should be around 0.9999 or 1. A value of zero for ncc indicates a complete uncorrelation between the original cover image and the watermarked image. Table-II ncc values are computed in all wavelet sub bands (LL, LH, HL, HH) of watermarked image. The watermarked medical image is subjected to six attack categories such as a 3×3 window mean filtering, a 3×3 window median filtering, 10°, 20°, 30° and 40° rotation, salt & pepper noise of noise densities 0.01,0.1,0.3 and 0.5, shear with x=0.5,y=0.5 and x=0,y=1, and finally crop with crop area [5,5], [50,50] and [100,100]. Table-II shows the robustness of lwt-svd under these attacks.

Table-II

Attacks	Magnetic Resonance Imaging(MRI) 'bd2'				Computer Tomography(CT) 'bd4'				Ultrasound (US) 'db6'			
	LL	LH	HL	HH	LL	LH	HL	HH	LL	LH	HL	HH
Mean Filtering (3×3)	0.9899	0.9789	0.9765	0.9799	0.9865	0.9854	0.9843	0.9811	0.9754	0.9786	0.9765	0.9654
Median Filtering (3×3)	0.8026	0.7916	0.7892	0.7926	0.7992	0.7981	0.797	0.7938	0.7881	0.7913	0.7892	0.7781
Rotation (10˚)	0.9776	0.9666	0.9642	0.9676	0.9742	0.9731	0.972	0.9688	0.9631	0.9663	0.9642	0.9531
Rotation (20˚)	0.9653	0.9543	0.9519	0.9553	0.9619	0.9608	0.9597	0.9565	0.9508	0.954	0.9519	0.9408
Rotation (30˚)	0.953	0.942	0.9396	0.943	0.9496	0.9485	0.9474	0.9442	0.9385	0.9417	0.9396	0.9285
Rotation (40˚)	0.9407	0.9297	0.9273	0.9307	0.9373	0.9362	0.9351	0.9319	0.9262	0.9294	0.9273	0.9162
Salt & Pepper Noise (density=0.01)	0.7007	0.6897	0.6873	0.6907	0.6973	0.6962	0.6951	0.6919	0.6862	0.6894	0.6873	0.6762
Salt & Pepper Noise (density=0.1)	0.6884	0.6774	0.675	0.6784	0.685	0.6839	0.6828	0.6796	0.6739	0.6771	0.675	0.6639
Salt & Pepper Noise (density=0.3)	0.6761	0.6651	0.6627	0.6661	0.6727	0.6716	0.6705	0.6673	0.6616	0.6648	0.6627	0.6516
Salt & Pepper Noise (density=0.5)	0.6638	0.6528	0.6504	0.6538	0.6604	0.6593	0.6582	0.655	0.6493	0.6525	0.6504	0.6393
Shear (x=0.5, y=0.5)	0.9456	0.9346	0.9322	0.9356	0.9422	0.9411	0.94	0.9368	0.9311	0.9343	0.9322	0.9211
Shear (x=0.2, y=0)	0.9443	0.9333	0.9309	0.9343	0.9409	0.9398	0.9387	0.9355	0.9298	0.933	0.9309	0.9198
Crop(5,5)	0.9913	0.9834	0.9776	0.981	0.9876	0.9865	0.9854	0.9822	0.9765	0.9797	0.9776	0.9665
Crop(50,50)	0.9784	0.9674	0.965	0.9684	0.975	0.9739	0.9728	0.9696	0.9639	0.9671	0.965	0.9539
Crop(100,100)	0.9677	0.9567	0.9543	0.9577	0.9643	0.9632	0.9621	0.9589	0.9532	0.9564	0.9543	0.9432

Six different types of attacks on the watermarked MRI image is shown in figure 13. Figure 13(a) gives 3×3 window mean attack, 13(b) median attack, figure 13(c) rotation attack, figure 13(d) noise attack, figure 13(e) shear attack and figure 13(f) shows crop attack on watermarked MRI image with patient data of size 64×64. The extracted watermark after attacks are shown in figure 14. Figure 15 shows attacks on watermarked CT images and figure 16 shows the extracted watermarks after attacks. Finally the US watermarked images are attacked and watermark extracted are shown in figure 17 and 18 respectively.

Comparing the figures 13 to figure 18 visually and computed ncc values in table-I of three types of medical cover image for 'bd2', 'db4' and 'db6' wavelets the following conclusions can be drawn.

One prominent conclusion is that the medical watermarked images get affected by noise in a remarkable manner compared to other attacks. This can be understood by observing the values form table-II where ncc for salt & pepper noise for all densities produced very poor results. Visually also 13(d), 15(d) and 17(d) the watermarked medical image is completely lost except for the edges. At the same time the extracted watermark from the noise attacked watermarked image is in good condition visually and the ncc is around 0.8223. Except noise attack, remaining attacks does not affect the proposed LWT-SVD watermarking and extraction processes. From the figures 14, 16 and 18 it can be visually noted that 'bd2' lifting wavelet scheme provides good quality extractions compared to 'db4' and 'db6' lifting schemes.
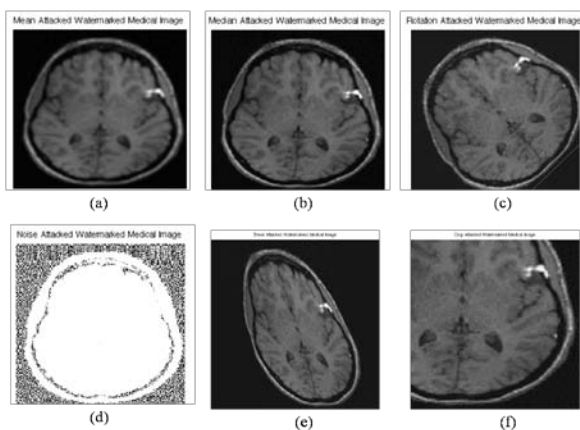
Fig.13. MRI Watermarked Images with 'db2' after (a) 3×3 window mean attack,(b) median attack,(c) rotation attack,(d) noise attack, (e) shear attack and (f) shows crop attacks
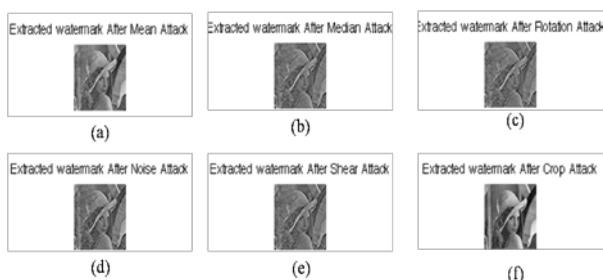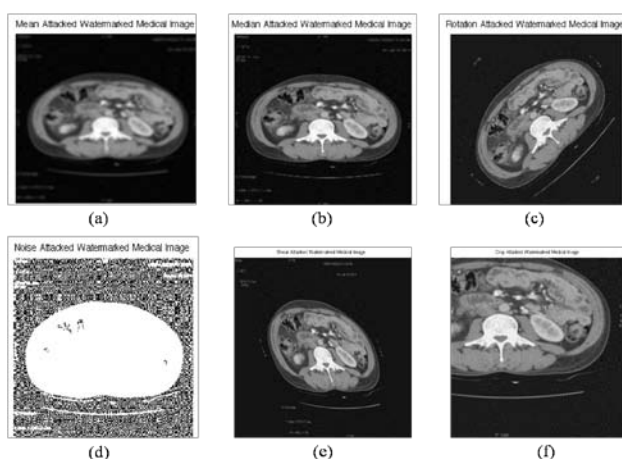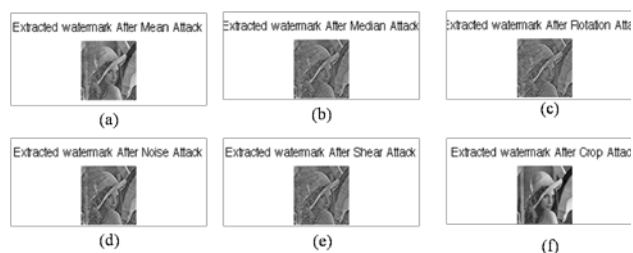

Fig.14. Extracted Patient images from MRI Watermarked Images with 'db2' after (a) 3×3 window mean attack,(b) median attack,(c) rotation attack,(d) noise attack, (e) shear attack and (f) shows crop attacks

Fig.15. CT Watermarked Images with 'db4' after (a) 3×3 window mean attack,(b) median attack,(c) rotation attack,(d) noise attack, (e) shear attack and (f) shows crop attacks

Fig.16. Extracted Patient images from CT Watermarked Images with 'db4' after (a) 3×3 window mean attack,(b) median attack,(c) rotation attack,(d) noise attack, (e) shear attack and (f) shows crop attacks
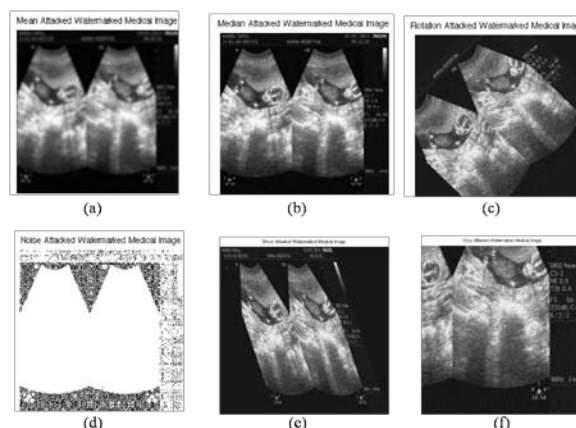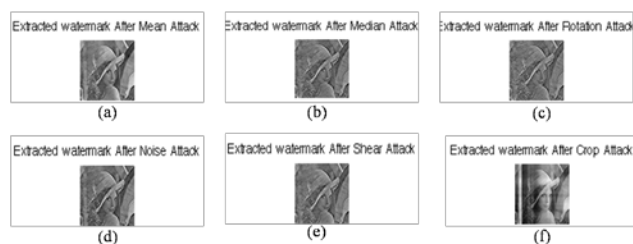

Fig.17. Ultrasound(US) Watermarked Images with 'db6' after (a) 3×3 window mean attack,(b) median attack,(c) rotation attack,(d) noise attack, (e) shear attack and (f) shows crop attacks

Fig.18. Extracted Patient images from US Watermarked Images with 'db6' after (a) 3×3 window mean attack,(b) median attack,(c) rotation attack,(d) noise attack, (e) shear attack and (f) shows crop attacks

Figure 19 plots the ncc values against attacks for MRI with 'db2', CT with 'db4' and US with 'db6' extracted patient images. The attacks are labeled on x-axis instead of full naming. The graph shows db2 and db4 mother wavelets perform well for lwt-svd watermarking procedures compared to db6.
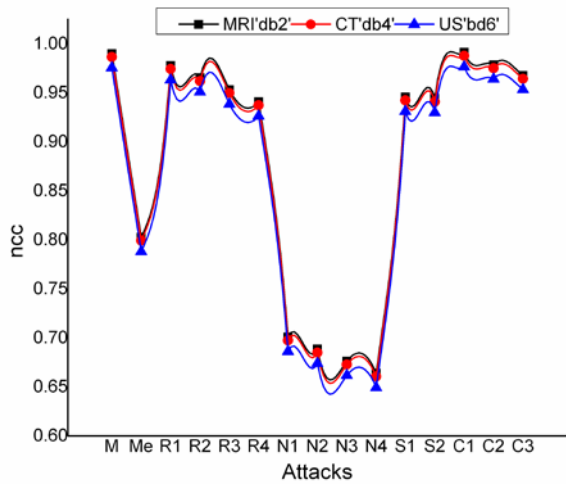
Fig.19. ncc of extracted patient images from MRI, CT and US Watermarked Images against attacks

Comparing dwt-svd watermarking procedure with lwt-svd technique for medical images using normalized cross correlation coefficient values, we found lwt-svd performs better the dwt-svd. The plot in figure 20 proves the above statement. The reason behind dwt's loss to lwt's lies in the inverse transformation which is an approximation process in case of dwt. The inverse process in lwt is ruination of the processes performed during the forward transformation which retains sensitive information in case of medical image watermarking. The rectangular marking show where dwt-svd failed to make an impression on medical image watermarking against attacks.
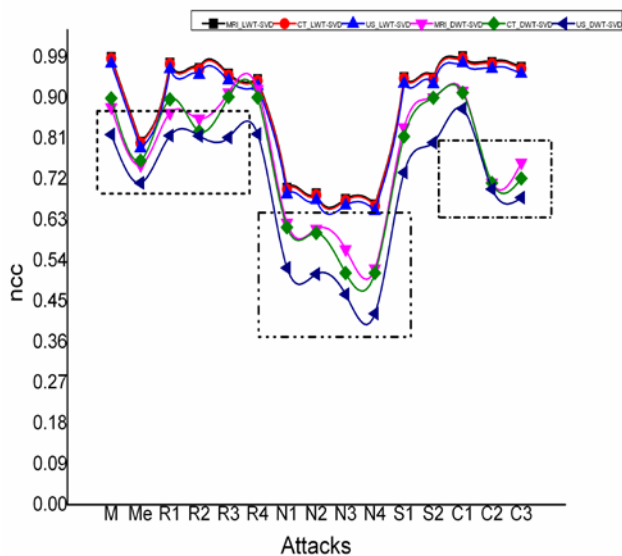

Fig.20. ncc of extracted patient images from MRI, CT and US Watermarked Images against attacks in case of dwt-svd and lwt-svd

Further the LWT-SVD based medical image watermarking process with 'db2' is tested by increasing the resolution of patient image to 256×256 which is equal to the resolution of the medical cover image. The patient images also include on top of the image their personal information regarding name, age, pervious medical history. Figure 21 shows the watermarked MRI and extracted patient image both of same resolution. Figure 22 and 23 show watermarked images and extracted images after attacks.
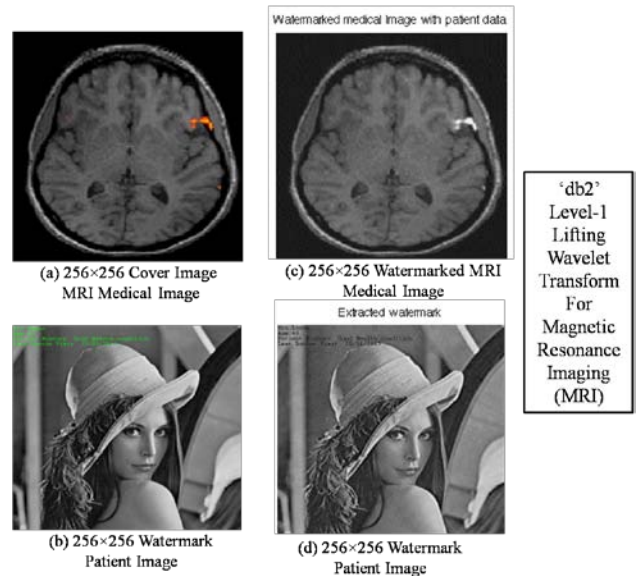

Fig.21. MRI Watermarked Images with 'db2' after (a) 256×256 cover image (b) 256×256 patient image as watermark,(c) 256×256 watermarked image,(d) 256×256 Extracted watermark
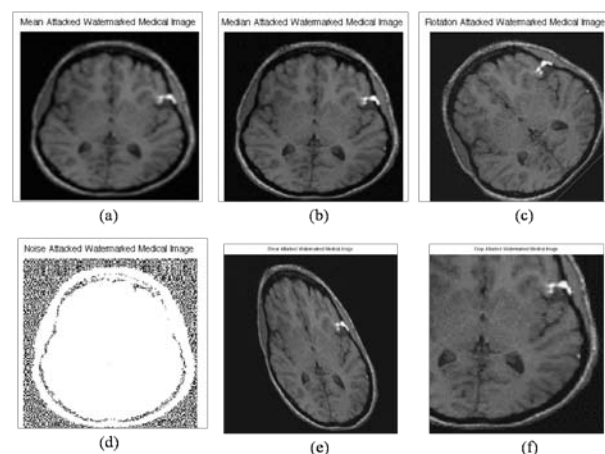

Fig.22. MRI Watermarked Images with 'db2' after (a) 3×3 window mean attack,(b) median attack,(c) rotation attack,(d) noise attack, (e) shear attack and (f) shows crop attacks

Fig.23. Extracted 256×256 Patient images from MRI Watermarked Images with 'db6' after (a) 3×3 window mean attack,(b) median attack,(c) rotation attack,(d) noise attack, (e) shear attack and (f) shows crop attacks
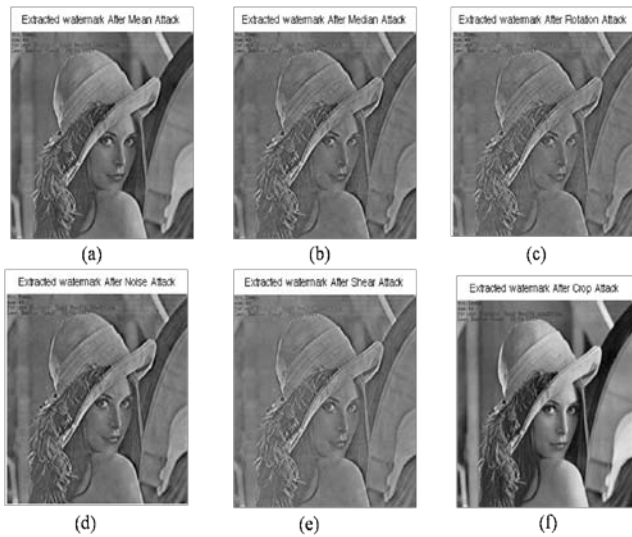
Similar procedure is repeated using CT images for a 256×256 patient image watermark with the proposed lwt-svd watermarking procedure. Figures 24 show the watermarked CT image and extracted patient image. Figures 25 and 26 show the attacks on the watermarked CT images and extraction of watermark patient images after attacks respectively.
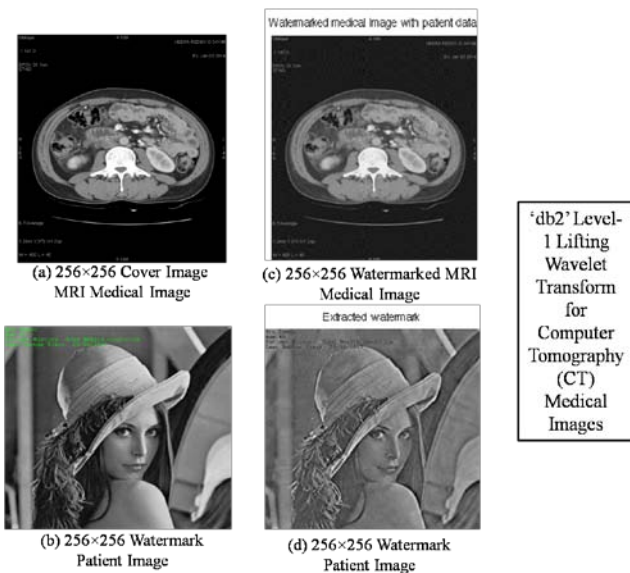

Fig.24. CT Watermarked Images with 'db2' after (a) 256×256 cover image (b) 256×256 patient image as watermark,(c) 256×256 watermarked image,(d) 256×256 Extracted watermark
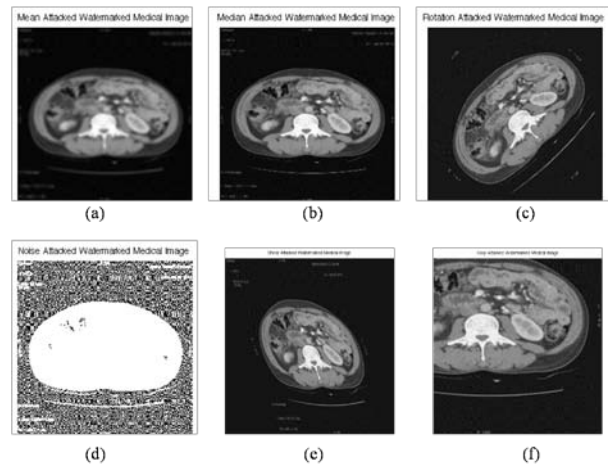

Fig.25. CT Watermarked Images with 'db2' after (a) 3×3 window mean attack,(b) median attack,(c) rotation attack,(d) noise attack, (e) shear attack and (f) shows crop attacks
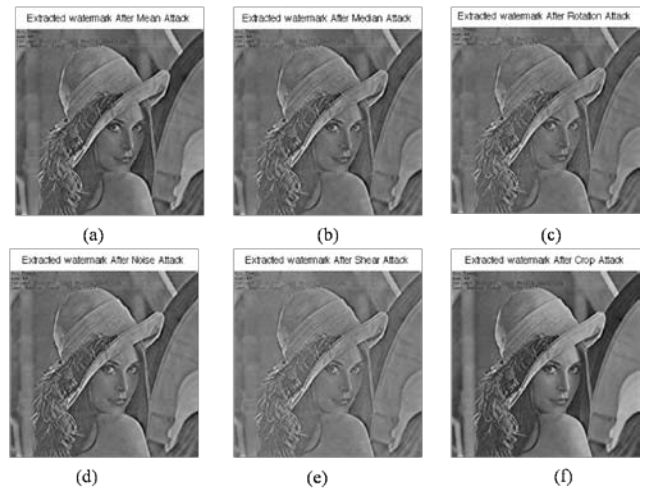

Fig.26. Extracted 256×256 Patient images from CT Watermarked Images with 'db6' after (a) 3×3 window mean attack,(b) median attack,(c) rotation attack,(d) noise attack, (e) shear attack and (f) shows crop attacks

5 Conclusion

In this paper lifting scheme of wavelet transform and singular value decomposition (LWT-SVD) is proposed for watermarking different types of medical images such as MRI,CT and US is proposed. In this method the singular values of the cover image are modified to create a watermarked medical image. Experimental results demonstrate that the lifting wavelet transform is a better prospect for medical image watermarking scheme compared to normal discrete wavelet transform. The results prove this fact visually and mathematically by computing psnr and ncc values.

Experiments are also performed by simulating the attacks which prove the robustness of the LWT-SVD method for medical image watermarking towards attacks. The proposed method does not put constraints on the resolution of the watermarks used.

References:

[1] Ruanaidh, Joseph JK, and Thierry Pun. "Rotation, scale and translation invariant spread spectrum digital image watermarking." *Signal processing* 66.3 (1998): 303-317.

[2] Swanson, Mitchell D., Bin Zhu, and Ahmed H. Tewfik. "Transparent robust image watermarking." *Image Processing, 1996. Proceedings., International Conference on*. Vol. 3. IEEE, 1996.

[3] Kundur, Deepa, and Dimitrios Hatzinakos. "A robust digital image watermarking method using wavelet-based fusion." *Image Processing, 1997. Proceedings., International Conference on*. Vol. 1. IEEE, 1997.

[4] Wong, Ping Wah, and Nasir Memon. "Secret and public key image watermarking schemes for image authentication and ownership verification."*Image Processing, IEEE Transactions on* 10.10 (2001): 1593-1601.

[5] Potdar, Vidyasagar M., Song Han, and Elizabeth Chang. "A survey of digital image watermarking techniques." *Industrial Informatics, 2005. INDIN'05. 2005 3rd IEEE International Conference on*. IEEE, 2005.

[6] Maity, Santi P., and Claude Delpha. "Optimization in digital watermarking techniques." *vol., Adv. techn. in multimedia watermarking: Image, video and audio appl., IGI Global Pub., USA* (2010): 369-406.

[7] Bors, Adrian G., and Ioannis Pitas. "Image watermarking using DCT domain constraints." *Image Processing, 1996. Proceedings., International Conference on*. Vol. 3. IEEE, 1996.

[8] Cox, Ingemar J., et al. "Secure spread spectrum watermarking for multimedia."*Image Processing, IEEE Transactions on* 6.12 (1997): 1673-1687.

[9] Bi, Ning, et al. "Robust image watermarking based on multiband wavelets and empirical mode decomposition." *Image Processing, IEEE Transactions on* 16.8 (2007): 1956-1966.

[10] Ganic, Emir, and Ahmet M. Eskicioglu. "Robust DWT-SVD domain image watermarking: embedding data in all frequencies." *Proceedings of the 2004 Workshop on Multimedia and Security*. ACM, 2004.

[11] Chandra, DV Satish. "Digital image watermarking using singular value decomposition." *Circuits and Systems, 2002. MWSCAS-2002. The 2002 45th Midwest Symposium on*. Vol. 3. IEEE, 2002.

[12] Mohamad Jansi, "PhD thesis 2005: Digital Watermarking in Medical Images", school of information systems, computing and Mathematics, Brunel University.

[13] Lou, Der-Chyuan, Ming-Chiang Hu, and Jiang-Lung Liu. "Multiple layer data hiding scheme for medical images." *Computer Standards & Interfaces* 31.2 (2009): 329-335.

[14] Tai, Wei-Liang, Chia-Ming Yeh, and Chin-Chen Chang. "Reversible data hiding based on histogram modification of pixel differences." *Circuits and Systems for Video Technology, IEEE Transactions on* 19.6 (2009): 906-910.

[15] Lavanya, A., and V. Natarajan. "Watermarking patient data in encrypted medical images." *Sadhana* 37.Part 6 (2012).

[16] Potdar, Vidyasagar M., Song Han, and Elizabeth Chang. "A survey of digital image watermarking techniques." *Industrial Informatics, 2005. INDIN'05. 2005 3rd IEEE International Conference on*. IEEE, 2005.

[17] D. Osborne, D. Rogers, J. Mazumdar, R. Coutts, D. Abbott, "An Overview of Wavelets for Image Processing for Wireless Applications", Proceedings of SPIE: Smart Structures, Devices and Systems, University of Melbourne, Australia, Vol. 4935, pp,427-435, 2002.

[18] Kishore, P. V. V., and P. Rajesh Kumar. "A Video Based Indian Sign Language Recognition System (INSLR) Using Wavelet Transform and Fuzzy Logic."*IACSIT International Journal of Engineering and Technology* 4.5 (2012).

[19] Kishore, P. V. V., et al. "Video Audio Interface for Recognizing Gestures of Indian Sign." *International Journal of Image Processing (IJIP)* 5.4 (2011): 479-503.

[20] Li, Qiang, Chun Yuan, and Yu-Zhuo Zhong. "Adaptive DWT-SVD domain image watermarking using human visual model." *Advanced Communication Technology, The 9th International Conference on*. Vol. 3. IEEE, 2007.

[21] Yavuz, Erkan, and Ziya Telatar. "Improved SVD-DWT based digital image

watermarking against watermark ambiguity." *Proceedings of the 2007 ACM symposium on Applied computing*. ACM, 2007.

[22] Li, Guohui, et al. "A sorted neighborhood approach for detecting duplicated regions in image forgeries based on DWT and SVD." *Multimedia and Expo, 2007 IEEE International Conference on*. IEEE, 2007.

[23] Yin, Cheng-qun, et al. "Color image watermarking algorithm based on DWT-SVD." *Automation and Logistics, 2007 IEEE International Conference on*. IEEE, 2007.

[24] Sweldens, "The lifting scheme: A construction of second generation wavelets." *SIAM Journal on Mathematical Analysis* 29.2 (1998): 511-546.

[25] Kumsawat, Prayoth, Kitti Attakitmongcol, and Arthit Srikaew. "An optimal robust digital image watermarking based on genetic algorithms in multiwavelet domain." *WSEAS Transactions on Signal Processing* 5.1 (2009): 42-51.

[26] Zhang, Yanhong. "Blind watermark algorithm based on HVS and RBF neural network in DWT domain." *Wseas transactions on computers* 8.1 (2009): 174-183.

[27] Venkatram, N., L. S. S. Reddy, and P. V. V. Kishore. "Multiresolution Medical Image Watermarking for Telemedicine Applications." *Digital Image Processing*6.1 (2014): 6-15.

[28] Kim, Kyung Hwan, and Sung June Kim. "A wavelet-based method for action potential detection from extracellular neural signal recording with low signal-to-noise ratio." *Biomedical Engineering, IEEE Transactions on* 50.8 (2003): 999-1011.